

Effect of optical wavelength on photoacoustic investigations of pulsatile blood flow

Tae-Hoon Bok, Eno Hysi, Michael C. Kolios*

Department of Physics, Ryerson University, 350 Victoria Street, Toronto, Ontario, M5B 2K3, Institute for Biomedical Engineering, Science and Technology, a partnership between Ryerson University and St. Michael's Hospital, Keenan Research Center for Biomedical Sciences of St. Michael's Hospital, 209 Victoria Street, Toronto, Ontario, M5B 1T8, Canada; mkolios@ryerson.ca

ABSTRACT

This paper attempts to experimentally and analytically quantify the aggregation-induced changes in the photoacoustic amplitude (PAA) by simultaneously examining the effect of red blood cell (RBC) aggregate size and optical illumination wavelength. In experiments, the pulsatile flow of human whole blood at 60 bpm was imaged using the VevoLAZR system equipped with a 40-MHz-linear-array probe. The samples were illuminated every 10 nm from 700 to 900 nm. For the analytical model, the PAA from both a collection of randomly distributed RBCs of 5, 10, 15, 20, 25, and 30 cells and a single absorber as a spherical aggregate of RBCs formed by the corresponding number of RBCs. The oxygen saturation (sO_2) was measured as 74% and 80% for the non-aggregated RBCs and the RBC aggregation. These values were assigned to the analytical RBC aggregates containing between 5 and 30 cells. The normalized PAA (nPAA) for the experimental results was compared to that generated by the theoretical calculations. At a given wavelength, the analytical nPAA for the collection of RBCs were identical for all numbers of RBCs, but that for the RBC aggregate increased with the number of RBCs forming the aggregate due to the increase in the effective photoacoustic absorber size. The experimental as well as analytical nPAA for both RBC aggregation and non-aggregation increased with the wavelength at a given absorber size. This was due to the fact that the PAA is mainly determined by the optical absorption coefficient (μ_a) which increases due to the relationship between ε_{HbO} and wavelength. In addition, the difference of PAA between RBC aggregation and non-aggregation also increased with the wavelength due to the increase in the μ_a induced by the hypothesized enhanced sO_2 resulting from the increased size of RBC aggregates. These results can be used as a means of estimating the oxygen loading and unloading during blood flow. This investigation elucidates the quantitative relationship between the RBC aggregate size and the optical illumination wavelength for probing the physiology of flowing blood.

Keywords: photoacoustics, red blood cell aggregation, oxygen saturation, optical wavelength dependence, isosbestic point, pulsatile blood flow

1. INTRODUCTION

The measurement of red blood cell (RBC) aggregation has been widely investigated, and most measurements are made under *in-vitro* conditions. Methods include the erythrocyte sedimentation rate¹, low shear viscometry², ultrasound (US) imaging³ and analysis of light transmission or reflection of RBC suspensions⁴. The behavior of RBC aggregation *in vivo* is much more complex compared to *in-vitro* conditions due to the structure of blood vessels, the dynamic compressibility of vessel wall, variable flow rates and vessel diameters, and the physiological condition of the individual. In order to non-invasively measure RBC aggregation *in vivo*, US imaging has been widely investigated^{3,5,6}. However, the US technique cannot provide functional aspects related to blood flow dynamics such as the oxygen delivery to tissues, a fundamental role of RBCs. In our group, photoacoustic (PA) imaging was proposed to simultaneously assess the changes in oxygen saturation (sO_2) due to RBC aggregation, under physiologically relevant pulsatile blood flow conditions⁷⁻¹⁰.

It is well established that the PA signal amplitude is dependent on the absorption coefficient (μ_a) and the size of the object¹¹. RBC aggregation in the normal human body is reversible phenomenon due to the cyclic change in the shear rate induced by blood flow velocity. The cyclic changes in shear rate result in the RBC aggregate size changing dynamically. In addition, it was reported that oxygen release was inhibited as RBCs aggregated^{12,13}. Inhibition of oxygen release results in

* mkolios@ryerson.ca

changes in the PA signal amplitude due to changes in relative number of oxygenated and deoxygenated hemoglobin molecules in the RBCs. The PA assessment of the relation between RBC aggregation and the sO₂ was studied by our group^{7,8}. Since the sO₂ is related to the molar concentration of oxygenated hemoglobin, the main factor impacting the μ_a ¹⁴, RBC aggregation inhibiting the oxygen release might be related to the μ_a . And, the μ_a is also a function of the molar extinction coefficient of oxygenated hemoglobin depending on the optical wavelength. Therefore, the complex relationship between RBC aggregation, the μ_a , and the optical wavelength should be investigated in a quantitative manner in order to better understand the PA assessment of blood flow and sO₂ measurements.

In the present paper, high-frequency PA imaging of whole blood flowing within a 2-mm-diameter vessel phantom was performed under the condition of pulsatile flow with the beat rate of 60 bpm. The blood flow was imaged by illuminating the sample from 700-900 nm at interval of 10 nm. Additionally, an analytical model was developed in order to simulate the PA amplitudes from both the collection of RBCs and their aggregates. The experimental results were also directly compared to the analytical findings.

2. MATERIALS AND METHODS

2.1 Blood flow system

Human blood was collected by netCAD (Vancouver, BC, Canada), the research division of Canadian Blood Services, under protocol 2013-001. Standard Canadian Blood Services collection and testing procedures of whole blood were followed. It was delivered overnight at 4°C, with continuous monitoring during shipment to ensure no temperature deviations occurred. The procedures for using the blood have been approved by the research ethics boards of Ryerson University and the Canadian Blood Services. Whole blood units from three different volunteers were used in order to ensure the repeatability of experimental results.

2.2 PA imaging and signal processing

The PA image was acquired by a VevoLAZR (FUJIFILM VisualSonics, Toronto, ON, Canada) US/PA system equipped with a 40 MHz linear-array probe under the pulsatile blood flow system developed by our group⁸. PA measurements were performed at 60 bpm for three blood samples at 21 optical wavelengths (λ) from 700 nm to 900 nm every 10 nm. For each measurement, 200 PA B-mode frames were recorded corresponding to a measurement time of 10 seconds at 20 fps frame rate. Out of the 200 frames, the 160 frames corresponding to 8 seconds were extracted and manually synchronized to the initial phase of the pulsatile cycle at each measurement.

Our group has previously shown that the PA amplitude (PAA) cyclically varied under pulsatile blood flow^{7,8}. Within the 8 seconds of measurement at 60 bpm, the PAA exhibited eight maximum (PAA_{max}, during the state of RBC aggregation) and eight minimum (PAA_{min}, during the state of disaggregation) as shown in Figure 1. The mean PAA_{max} and the mean PAA_{min} were computed as a function of optical wavelength. In order to compare the experimental PAA with the theoretical equivalent, they were normalized to the norm of the mean PAA_{min} for every optical wavelength. The PAA_{min} was recorded during the phase of disaggregation (i.e. collection of RBCs). The normalized PAA for the experimental results (nPAA_e) at each wavelength can be expressed as,

$$nPAA_{e, X} |_{\lambda_n} = \frac{mean(PAA_X) |_{\lambda_n}}{\sqrt{\sum_{n=700nm}^{900nm} (mean(PAA_{min}) |_{\lambda_n})^2}}, (n = 700, 710, \dots, 900 \text{ nm}) \quad (1)$$

where the subscript X indicates max or min, nPAA_{e,max} or nPAA_{e,min}, respectively.

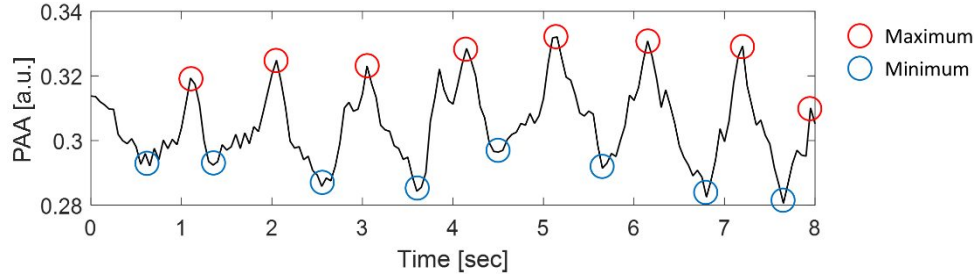


Figure 1. Cyclic variation in photoacoustic amplitude (representative at 850 nm of the optical wavelength). The eight PAA_{\max} as well as eight PAA_{\min} were averaged to compute Equation (1).

2.3 PA modeling of RBC aggregation

The time dependent PA pressure field for a uniformly irradiated spherical absorber can be expressed as¹¹,

$$p_s(r, t) = \frac{i\mu_a \beta F v_s^2 a}{2\pi C_p r} \int_{-\infty}^{\infty} \frac{(\sin \hat{q} - \hat{q} \cos \hat{q}) e^{ik_f(r-a-v_f t)}}{\hat{q}^2 [(1-\hat{\rho})(\sin \hat{q}) / \hat{q} - \cos \hat{q} + i\hat{q}\hat{v} \sin \hat{q}]} d\omega, \quad (2)$$

where r is the distance between the absorber and the ultrasonic detector, t is time, μ_a is the optical absorption coefficient, β is the isobaric thermal expansion coefficient, F is the optical fluence of the excitation light, v_s is the sound speed in the absorber, a is the radius of the uniformly irradiated spherical absorber, C_p is the heat capacity per unit mass, \hat{q} is defined as $\hat{q} = \omega a / v_s$, where ω is the modulation frequency of the optical source, k_f and v_f are the acoustic wave number and sound speed within the surrounding fluid medium, respectively, $\hat{\rho}$ and \hat{v} are the ratios of density (ρ_s / ρ_f) and the sound speed (v_s / v_f), respectively, where ρ_s and ρ_f are the density of the absorber and the surrounding fluid medium, respectively.

In the case where a collection of spherical absorbers is present within the region of interest (ROI), assuming that the incident optical intensity is the same for all absorbers within the ROI, the linear superposition principle can be applied to retrieve the resultant PA pressure field from the ROI. It is given by¹⁵,

$$p_M(r, t) = \frac{i\mu_a \beta F v_s^2 a}{2\pi C_p r} \int_{-\infty}^{\infty} \frac{(\sin \hat{q} - \hat{q} \cos \hat{q}) e^{ik_f(r-a-v_f t)}}{\hat{q}^2 [(1-\hat{\rho})(\sin \hat{q}) / \hat{q} - \cos \hat{q} + i\hat{q}\hat{v} \sin \hat{q}]} \sum_{m=1}^M e^{-ik_f \cdot r_m} d\omega, \quad (3)$$

where M is the number of RBCs, k_f is defined by the direction of observation, and r_m stands for the position vector of the m th absorber. The position of each RBC was assumed to be randomly distributed in 2 dimensions. The random position for each RBC was iterated 10 times, so that p_M was computed 10 times with the 10 cases of RBC positions. The distance between adjacent RBCs was adjusted so that the total hematocrit of the sample was 40 %. Equation (2) and (3) describe an analytic signal which contains all possible frequencies generated, i.e. it is non-bandlimited.

In practical measurements, bandlimited (BL) ultrasonic transducers are used to receive the PA signals. As such, Equations (2) and (3) were converted into the BL analytic PA signals for the single absorber (P_s) and the collection of absorbers (P_M), respectively^{16,17},

$$P_s(r, t) = \text{Re}(p_s(r, t)) \otimes h(t) + i \text{Re}(p_s(r, t)) \otimes \tilde{h}(t), \quad (4)$$

$$P_M(r, t) = \text{Re}(p_M(r, t)) \otimes h(t) + i \text{Re}(p_M(r, t)) \otimes \tilde{h}(t), \quad (5)$$

where \otimes represents the convolution operator, and $h(t)$ is the impulse response of the receiver. Assuming that the frequency response profile of a transducer can be modeled as a Gaussian function¹⁸, $h(t)$ can be written as,

$$h(t) = \text{Re} \left(\frac{1}{2\pi} \int_{-\infty}^{\infty} e^{-(\omega-\omega_0)^2 / 2\sigma^2} e^{i\omega t} d\omega \right) = \frac{\sigma}{\sqrt{2\pi}} e^{-\sigma^2 t^2 / 2} \cos(\omega_0 t), \quad (6)$$

$$\tilde{h}(t) = \text{Im} \left(\frac{1}{2\pi} \int_{-\infty}^{\infty} e^{-(\omega-\omega_0)^2/2\sigma^2} e^{i\omega t} d\omega \right) = \frac{\sigma}{\sqrt{2\pi}} e^{-\sigma^2 t^2/2} \sin(\omega_0 t), \quad (7)$$

where σ is the -6 dB bandwidth of the receiver, ω_0 is the central frequency of the transducer.

In order to simulate RBC aggregates from collections of RBCs, the equivalent radius (a_{eq}) of the largest, single spherical aggregate that could be formed within a sample could be computed by $a_{eq} = (3V/(4\pi))^{1/3}$, where V is the equivalent volume of the aggregate. Equations (4) and (5) were then used in order to obtain the BL, analytical PAA for both the spherical aggregate of RBCs ($P_{M,AG} = P_s$) and the collection of non-aggregated RBCs ($P_{M,NA}$), respectively. The analytic PAA was normalized to the norm of the $P_{M,NA}$ for all optical wavelengths in order to compare with the experimental equivalent measurement, nPAA_e. The normalized PAA for the analytic results at each wavelength can be expressed as,

$$\text{nPAA}_{M,AG} \Big|_{\lambda_n} = \frac{P_{M,AG} \Big|_{\lambda_n}}{\sqrt{\sum_{n=700nm}^{900nm} \left(P_{M,NA} \Big|_{\lambda_n} \right)^2}}, \quad (n = 700, 710, \dots, 900 \text{ nm}) \quad (8)$$

$$\text{nPAA}_{M,NA} \Big|_{\lambda_n} = \frac{P_{M,NA} \Big|_{\lambda_n}}{\sqrt{\sum_{n=700nm}^{900nm} \left(P_{M,NA} \Big|_{\lambda_n} \right)^2}}, \quad (n = 700, 710, \dots, 900 \text{ nm}) \quad (9)$$

where the subscript *AG* and *NA* represent the aggregate and the collection of non-aggregated RBCs, respectively. The number of RBCs were arbitrary taken by increments of 5 cells from 5 to 30 cells. This is since 4 to 10 cells normally form an aggregate and aggregates containing more than 10 cells are infrequently observed^{19,20}.

2.4 Estimating the μ_a from experimentally measured sO₂

Assuming that the oxygenated (HbO) and deoxygenated (Hb) hemoglobin were the dominant absorbers in a RBC, the sO₂ was estimated by

$$sO_2 = \frac{[\text{HbO}]}{[\text{HbO}] + [\text{Hb}]} = \frac{\text{PAA}_{\lambda_2} \varepsilon_{\text{Hb}}^{\lambda_1} - \text{PAA}_{\lambda_1} \varepsilon_{\text{Hb}}^{\lambda_2}}{\text{PAA}_{\lambda_1} (\varepsilon_{\text{HbO}}^{\lambda_2} - \varepsilon_{\text{Hb}}^{\lambda_2}) - \text{PAA}_{\lambda_2} (\varepsilon_{\text{HbO}}^{\lambda_1} - \varepsilon_{\text{Hb}}^{\lambda_1})}, \quad (10)$$

where [HbO] and [Hb] are the molar concentration of HbO and Hb, respectively, λ_1 and λ_2 are the shorter and longer wavelengths than an isosbestic point (800 nm), respectively, ε_{HbO} and ε_{Hb} are the molar extinction coefficient of HbO and Hb, respectively. μ_a is governed by both [HbO] and [Hb] such as $\mu_a = \varepsilon_{\text{HbO}}[\text{HbO}] + \varepsilon_{\text{Hb}}[\text{Hb}]$ ¹⁴. At a given optical wavelength, the μ_a of a blood sample (single or aggregated) can be dependent on the sO₂ since [HbO] is proportional to the sO₂,

$$\mu_a \approx (\varepsilon_{\text{HbO}} - \varepsilon_{\text{Hb}}) sO_2 + \varepsilon_{\text{Hb}}, \quad (11)$$

In our previous studies, we showed that the sO₂ varied from 74% to 80% during one pulsatile cycle. We hypothesized this is a result to the changes in the RBC aggregation level as a function of the pulsatile cycle^{12,13}. Hence, the sO₂ of the RBC aggregate formed by the number of RBCs ranging from 5 to 30 cells for Equation (10) were assumed to range between 75% and 80%, at intervals of 1%. The sO₂ of the non-aggregated RBCs was assumed as 74%. The nPAA was computed considering Equations (8) and (9) with respect to the varying sO₂ at each wavelength from 700 to 900 nm every 10 nm.

2.5 Normalized magnitude of variation in nPAA (nVnPAA)

The magnitude of variation in nPAA for the analytic results ($\text{VnPAA}_M = \text{nPAA}_{M,AG} - \text{nPAA}_{M,NA}$) as well as the experimental magnitude of variation ($\text{VnPAA}_{\text{exp}} = \text{nPAA}_{\text{e,max}} - \text{nPAA}_{\text{e,min}}$) can represent the degree of RBC aggregation. In order to compare the VnPAA_M to the $\text{VnPAA}_{\text{exp}}$ as a function of a particular wavelength, the VnPAA at each wavelength was normalized to the norm of the VnPAA depending on the wavelength, expressed by,

$$nVnPAA_{\text{exp}}|_{\lambda_n} = \frac{VnPAA_{\text{exp}}|_{\lambda_n}}{\sqrt{\sum_{n=700nm}^{900nm} \left(VnPAA_{\text{exp}}|_{\lambda_n} \right)^2}}, \quad (n = 700, 710, \dots, 900 \text{ nm}) \quad (12)$$

$$nVnPAA_M|_{\lambda_n} = \frac{VnPAA_M|_{\lambda_n}}{\sqrt{\sum_{n=700nm}^{900nm} \left(VnPAA_M|_{\lambda_n} \right)^2}}, \quad (n = 700, 710, \dots, 900 \text{ nm}) \quad (13)$$

3. RESULTS AND DISCUSSION

The nPAA as a function of the wavelength for the analytic and the experimental results were shown in Figure 2b. The nPAA from the collection of the non-aggregated RBCs ($nPAA_{M,NA}$, thin lines) increased with the wavelength. This is consistent with the relation between ε_{HbO} and the wavelength (Figure 2a) and can be explained from the fact that the blood is at least 75% oxygenated. In addition, the $nPAA_{M,NA}$ were almost identical for all cases of the number of RBCs. This suggested that the ratio of the PAA at each wavelength to the magnitude of the PAA as a function of the wavelength remained the same even though the number of RBCs was changed. Such an observation was a result of the fact that the nPAA was normalized by all wavelengths of illumination. The $p_{M,NA}$ increased with the number of RBCs (not shown in this paper).

The nPAA from the spherically aggregated single absorber ($nPAA_{M,AG}$, thick lines) increased with not only the wavelength but also the aggregate size which is related to the number of RBCs present within a single aggregate. This is because the PAA is a function of the absorber size as well as the μ_a in Equation (2). In the experimental results, the maximal amplitude in nPAA ($nPAA_{e,\text{max}}$) as well as the minimal one ($nPAA_{e,\text{min}}$) increased with the wavelength. This is in agreement with the analytical results. However, the difference between $nPAA_{e,\text{max}}$ and $nPAA_{e,\text{min}}$ is smaller than those between $nPAA_{M,AG}$ and $nPAA_{M,NA}$ except for the case of 5 cells. In the experiments, the RBCs were flowing with a flow rate of 75 ml/min and a beat rate of 60 bpm. As a result, the aggregation tendency during this condition was much lower than that under the condition of RBCs that are static or have a very low flow velocity. At a given wavelength, the difference between the $nPAA_{M,AG}$ and $nPAA_{M,NA}$ increased with the number of RBCs since the absorber size plays a significant role. As the number of RBCs increased, the difference between the $nPAA_{M,AG}$ and $nPAA_{M,NA}$ increased with wavelength, which resulted in increases in the slope of the $nPAA_{M,AG}$ as a function of the wavelength (Figure 2b).

The PAA is a function of the absorber size and optical absorption at a given wavelength, so that the VnPAA is a function of the magnitude of variation in both the absorber size (Δa) and the μ_a ($\Delta\mu_a$). $\Delta\mu_a$ represents the difference in the μ_a between the aggregate and the collection of non-aggregated RBCs. If the RBC aggregation-induced change in the sO_2 is not considered (meaning that μ_a is independent of the sO_2), then the VnPAA should be wavelength independent. However, as the aggregate size increases, the sO_2 also becomes higher when compared to the non-aggregated RBCs^{12,13}. Consequently, the μ_a also increases by means of Equation (11). The increased μ_a (due to changes in the ratio of oxygenated and deoxygenated Hb at difference aggregation levels) as well as the increased absorber size induced by RBC aggregation, should enhance the VnPAA as a function of optical wavelength.

For the smallest number of RBCs in an aggregate, 5 cells (blue lines), the simulation results as a function of wavelength (the difference between the $nPAA_{M,AG}$ and $nPAA_{M,NA}$ for each wavelength) and experimental results (the difference between the $nPAA_{e,\text{max}}$ and $nPAA_{e,\text{min}}$, black line) are comparable. In order to compare those differences for all cases, the nVnPAA were plotted in Figure 2c. The difference between nPAA for the experimental results ($nVnPAA_{\text{exp}}$) as well as the analytical one ($nVnPAA_M$) increased with the wavelength. This result is due to the fact that the RBC aggregation increased the sO_2 , which in turn affected the μ_a , resulting in the increase in the $VnPAA_{\text{exp}}$ as a function of wavelength.

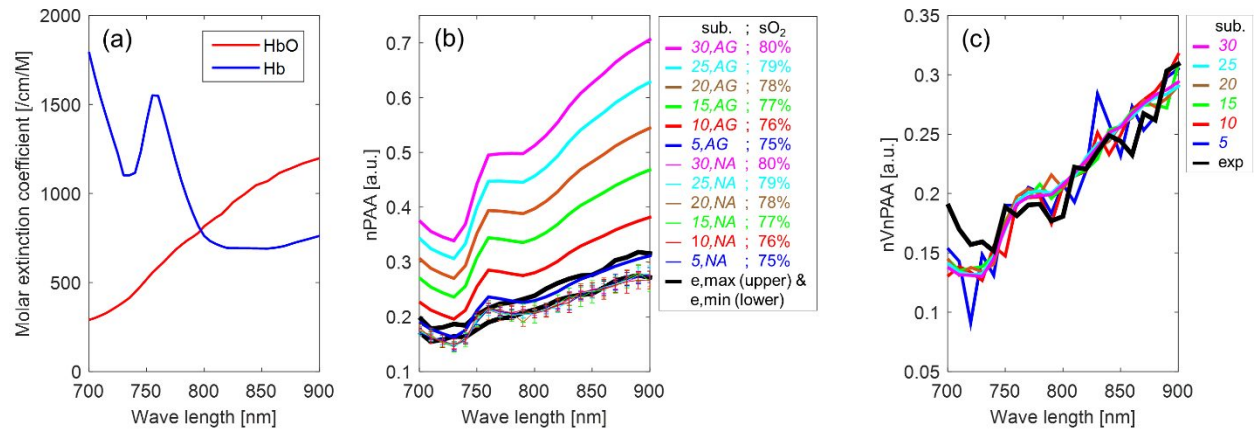


Figure 2. (a) Molar extinction coefficient of oxygenated (HbO) and deoxygenated (Hb) hemoglobin as a function of the wavelength²¹. (b) The normalized photoacoustic amplitude of the analytic ($nPAA_{M,AG}$ for the single absorber as a spherical aggregate formed by the number of RBCs expressed as M and $nPAA_{M,NA}$ for the collection of the number of RBCs) and the experimental ($nPAA_{e,max}$ & $nPAA_{e,min}$) results. The error bars indicate the standard deviation for the iteration time ($n=10$) of $nPAA_{M,NA}$ for the random distribution of the non-aggregated RBCs. (c) The normalized magnitudes of the differences between the $nPAA_{M,AG}$ and $nPAA_{M,NA}$ for the analytic results, and between $nPAA_{e,max}$ and $nPAA_{e,min}$ for the experimental results.

4. CONCLUSION

The PAA was measured as a function of the optical wavelength under the pulsatile blood flow in order to investigate the cyclic variation in RBC aggregation. An analytical expression for the PA signal from collections of single cells and aggregates of RBCs was derived by varying the number of RBCs in an aggregate from 5 to 30 cells. The experimental as well as the analytic PAA in the presence of RBC aggregation and non-aggregation increased with the wavelength due to the increase in ϵ_{HbO} depending on the wavelength. In addition, the difference of PAA between the phase of RBC aggregation and non-aggregation also increased with the wavelength due to the increase in the μ_a induced by the enhanced sO₂ resulting from the increased size of RBC aggregate. Even though the degree of RBC aggregation under pulsatile blood flow are consistent in nature, its measured level such as the PAA can be dependent on the optical wavelength. As such, the relation between RBC aggregation and the sO₂ in terms of PA measurement should be further quantitatively investigated.

REFERENCES

- [1] Erikssen, G., Liestøl, K., Bjørnholt, J. V., Stormorken, H., Thaulow, E., Erikssen, J., "Erythrocyte sedimentation rate: a possible marker of atherosclerosis and a strong predictor of coronary heart disease mortality," *Eur. Heart J.* **21**(19), 1614–1620 (2000).
- [2] Brooks, D. E., Goodwin, J. W., Seaman, G. V. F., "Rheology of erythrocyte suspensions: electrostatic factors in the dextranmediated aggregation of erythrocytes," *Biorheology* **11**, 69–76 (1974).
- [3] Cloutier, G., Qin, Z., "Ultrasound backscattering from non-aggregating and aggregating erythrocytes-a review," *Biorheology* **34**(6), 443–470 (1997).
- [4] Hardeman, M. R., Dobbe, J. G. G., Ince, C., "The laser-assisted optical rotational cell analyzer (LORCA) as red blood cell aggregometer," *Clin. Hemorheol. Microcirc.* **25**, 1–11 (2001).
- [5] Bok, T.-H., Li, Y., Nam, K.-H., Choi, J. C., Paeng, D.-G., "Feasibility study of high-frequency ultrasonic blood imaging in human radial artery," *J. Med. Biol. Eng.* **35**(1), 21–27 (2015).
- [6] Paeng, D. G., Nam, K. H., Shung, K. K., "Cyclic and radial variation of the echogenicity of blood in human carotid arteries observed by harmonic imaging," *Ultrasound Med. Biol.* **36**(7), 1118–1124 (2010).
- [7] Bok, T.-H., Hysi, E., Kolios, M. C., "Simultaneous measurement of erythrocyte aggregation and oxygen saturation

- under in vitro pulsatile blood flow by high-frequency photoacoustics,” 2014 IEEE Int. Ultrason. Symp. Proc., 1292–1295, Chicago, IL, USA (2014).
- [8] Bok, T.-H., Hysi, E., Kolios, M. C., “High-frequency photoacoustic imaging of erythrocyte aggregation and oxygen saturation: probing hemodynamic relations under pulsatile blood flow,” Proc. SPIE **9323**, 93231Q, San Francisco, CA, USA (2015).
- [9] Hysi, E., Saha, R. K., Kolios, M. C., “Photoacoustic ultrasound spectroscopy for assessing red blood cell aggregation and oxygenation,” J. Biomed. Opt. **17**(12), 125006–125010 (2012).
- [10] Hysi, E., Saha, R. K., Kolios, M. C., “On the use of photoacoustics to detect red blood cell aggregation,” Biomed. Opt. Express **3**(9), 2326–2338 (2012).
- [11] Diebold, G. J., “Photoacoustic monopole radiation: waves from objects with symmetry in one, two and three dimensions,” [Photoacoustic Imaging and Spectroscopy], L. V. Wang, Ed., CRC Press, Boca Raton, FL, 3–17 (2009).
- [12] Tateishi, N., Suzuki, Y., Shirai, M., Cicha, I., Maeda, N., “Reduced oxygen release from erythrocytes by the acceleration-induced flow shift, observed in an oxygen-permeable narrow tube,” J. Biomech. **35**(9), 1241–1251 (2002).
- [13] Tateishi, N., Suzuki, Y., Cicha, I., Maeda, N., “O₂ release from erythrocytes flowing in a narrow O₂-permeable tube: effects of erythrocyte aggregation,” Am. J. Physiol. - Hear. Circ. Physiol. **281**(1), H448–H456 (2001).
- [14] Wang, X., Xie, X., Ku, G., Wang, L. V., Stoica, G., “Noninvasive imaging of hemoglobin concentration and oxygenation in the rat brain using high-resolution photoacoustic tomography,” J. Biomed. Opt. **11**(2), 24015–24019 (2006).
- [15] Saha, R. K., Kolios, M. C., “A simulation study on photoacoustic signals from red blood cells,” J. Acoust. Soc. Am. **129**(5), 2935–2943 (2011).
- [16] Bracewell, R. N., The Fourier Transform And Its Applications, McGraw-Hill, Singapore (2000).
- [17] Saha, R. K., Karmakar, S., Roy, M., “Computational investigation on the photoacoustics of malaria infected red blood cells,” PLoS One **7**(12), 1–9 (2012).
- [18] Szabo, T. L., Diagnostic Ultrasound Imaging: Inside Out, Elsevier Academic Press, New York, NY (2004).
- [19] Segen, J. C., “Concise Dictionary of Modern Medicine,” 2006, <<http://medical-dictionary.thefreedictionary.com/rouleaux>>.
- [20] Pop, C. V. L., Neamtu, S., “Aggregation of red blood cells in suspension: study by light-scattering technique at small angles,” J. Biomed. Opt. **13**(4), 041308 (2011).
- [21] Prah, S., “Optical Absorption of Hemoglobin,” 2015, <<http://omlc.org/spectra/hemoglobin/>>.